Turkish Journal of Electrical Engineering & Computer Sciences

http://journals.tubitak.gov.tr/elektrik/

Research Article

Turk J Elec Eng & Comp Sci
(2017) 25: 3881 – 3891

doi:10.3906/elk-1607-314

Experimental analysis of the temperature dependence of the Brillouin gain spectrum in short-length single-mode fiber

Murat YÜCEL[1,*], Halim Haldun GÖKTAŞ[2], Murat YÜCEL[3], Nail Ferhat ÖZTÜRK[4], Abdullah Erkam GÜNDÜZ[2]

[1]Department of Electrical & Electronics Engineering, Faculty of Technology, Gazi University, Ankara, Turkey

[2]Department of Electrical & Electronics Engineering, Faculty of Engineering and Natural Sciences, Yıldırım Beyazıt University, Ankara, Turkey

[3]Department of Electrical & Electronics Technology, Yenimahalle Vocational and Technical Anatolian High School, Ankara, Turkey

[4]Turkish State Railways, Ankara, Turkey

Received: 27.07.2017 • **Accepted/Published Online:** 07.04.2017 • **Final Version:** 05.10.2017

Abstract: The Brillouin backscattered wave was examined in a short-length single-mode fiber at different ambient temperatures using a 1553-nm wavelength laser source. To obtain Brillouin scattering depending on the temperature change in a 95-m long single-mode fiber cable, the Brillouin optical time domain reflectometry (BOTDR) technique was used. In this technique, a 1553 nm wavelength signal was sent from one side of the test fiber. The FC/APC connector was attached to the other end of the test fiber. The temperature parameters of the single-mode fiber cables of different brands and types can be obtained using Brillouin scattering. The Brillouin frequency shift is found 0.93 MHz/°C. Measured linear change demonstrated its use as the temperature sensor of Brillouin Scattering.

Key words: Brillouin scattering, Brillouin optical time domain reflectometry, temperature dependence

1. Introduction

Scattering is dispersion formed by the incident beam hitting a foreign object and resulting in light loss. The most important scatterings are Rayleigh scattering (linear), Brillouin scattering, and Raman scattering (nonlinear) in the fiber optic cable [1,2].

Rayleigh scattering occurs when particles are small compared to the wavelength of the light, caused by random inhomogeneities. Raman scattering emerges as a result of the interaction between the molecular vibrational modes occurring in the molecular structure of the medium with the emitted light within the fiber. Brillouin scattering, with the heat coming from the light wave in the fiber, occurs spontaneously as a result of the interaction of acoustic waves [3,4].

Optical fibers are widely used for data transmission and in physical sensing systems. For the last 30 years, fiber optic sensors have become the subject of many interesting studies and various sensors have been developed for the measurement of chemical and physical factors. In physical sensing applications, the changes in refractive index and geometric properties are observed to monitor temperature, strain, and pressure [5].

The compact size, low setup and maintenance costs, and electromagnetic interference (EMI) invulnera-

*Correspondence: muyucel@gazi.edu.tr

bility make optical sensors a very competitive and desirable choice compared to other classical sensors. Fiber optic sensors allow for monitoring of very large areas with a simple, small monitoring station that basically has the size of a normal desktop PC. Hence, a single fiber sensor can do all the monitoring done by many separate classical sensors by itself. The distributed fiber sensors provide even more flexibility since basically all of the fibers become a sensing point. Therefore, distributed sensors are commonly used in many hard to monitor media such as railroads, bridges, tunnels, oil pipelines, and borders [6].

The concept of the distributed fiber sensor was firstly developed by Southampton University in 1981 [7,8]. Later, Hartog and Payne developed the concept further [9]. They managed to obtain the Rayleigh scattering temperature coefficient along a liquid core silica fiber. Dakin et al. managed to monitor temperature by using the anti-Stokes and Stokes Raman backscattering coefficients [10]. Following the studies by Hartog and Dakin, these types of sensors have seen rapid development [11,12]. In 1989, the Brillouin frequency shift was reported to change with temperature and strain [13,14]. From then on, Brillouin scattering has been important for distributed fiber optic sensors since strain is an important factor for fibers and is a necessity for monitoring the structural integrity of big constructions. Furthermore, the range of Brillouin sensors is quite big because the Brillouin frequency shift is small (approximately 11 GHz) compared to Raman and it can be used in the 1550 nm band with minimum fiber loss. However, in Raman scattering, the pump/Stokes and Anti-stokes waves cannot coexist at this wavelength band. In order to elongate the range of distributed sensors, fiber-based Brillouin lasers [15] and amplifiers [16] were designed [17,18]. Some special monitoring applications require sensor systems with a much greater range than distributed optical sensors [19,20]. Some examples of such applications are power plants, fire monitoring systems, coal mines, oil well safety, high-speed train lines, and long railroad network safety [21]. Rayleigh and Raman scattering-based distributed fiber optic temperature sensors are used in tunnels, subways, the iron and steel sector, petro-chemistry factories, and other hazardous and hard to reach places. Their main use is for fire protection [22,23]. However, these distributed sensors have very limited sensitivity. Due to weak wave signals, as the sensing range increases, the response time increases as well. Thanks to the important studies on the fiber length and resolution over the past decade, Brillouin scattering has become the most important scattering technique used for distributed fiber optic sensing.

Brillouin gain spectrum (BGS) is enhanced by the fiber length increases. Therefore, there are studies in the literature for more fiber length of 250 m and above. With this study, BGS analysis was performed for a much shorter fiber size. Brillouin scattering is examined in the 95 m single-mode fiber at different ambient temperatures. In the second part of the study, the theoretical calculations of distributed Brillouin sensors are studied. In the third part, the experimental observation of Brillouin scattering in single-mode fiber is performed.

2. Theoretical analysis

As the wave propagates through the optical fiber, a small amount is scattered back due to the Brillouin interaction. As shown in Figure 1, this backscattering can have a frequency either lower (Stokes) or higher (anti-Stokes) than the incident wave.

When an electric field oscillates at the pump frequency known as ω_0 then the electrostriction process produces a macroscopic acoustic wave at the frequency ω_B. In spontaneous Brillouin scattering, pump photons are suppressed. This results in the creation of a Stokes photon and an acoustic phonon concurrently. The energy conservation and momentum conservation (MC) must be followed in similar scattering processes. For conservation of energy,

$$\omega_0 = \omega_s + \omega_B, \tag{1}$$

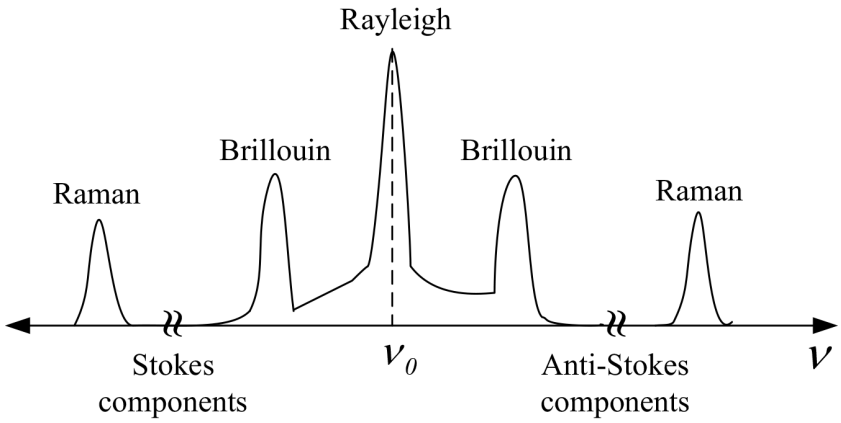

Figure 1. Rayleigh, Brillouin and Raman scatterings.

where ω_s is the frequency of Stokes shift. For MC,

$$k_0 = k_s + k_B \tag{2}$$

k_0, k_s, and k_B represent momentum vectors of the incident wave, scattered Stokes wave, and acoustic wave, respectively. As shown in Figure 2, the frequency and wave numbers are related to the dispersion for acoustic and electromagnetic waves:

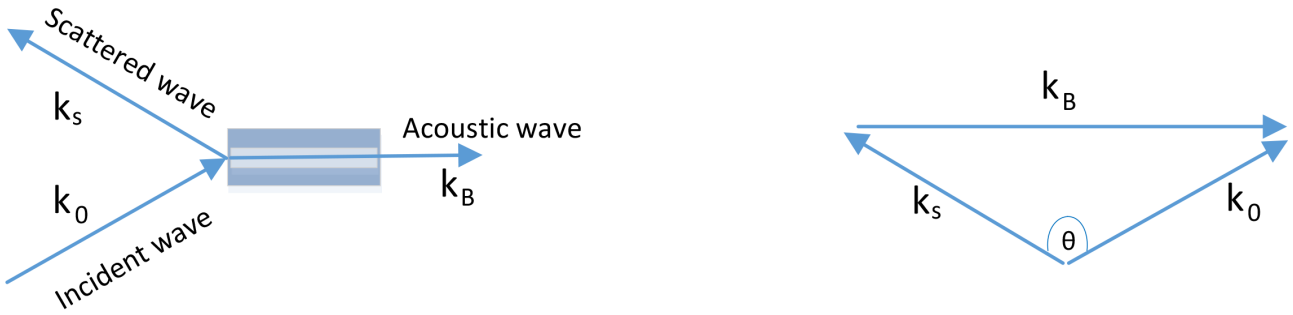

Figure 2. Formation of the Stokes components of the Brillouin scattering [6].

$$|k_0| = \frac{n\omega_0}{c} |k_s| = \frac{n\omega_s}{c} |k_B| = \frac{\omega_B}{V_A}, \tag{3}$$

where c is the speed of light in a vacuum, n is the refractive index, and V_A is the acoustic velocity.

In a mass medium, scattering occurs in every direction. Using Eqs. (**??**) and (**??**), the angular frequency of the acoustic wave can be calculated with the following equation:

$$\omega_B \approx 2V_A |k_0| \sin\left(\frac{\theta}{2}\right) \tag{4}$$

θ is the angle between the incident and Stokes waves. Eq. (**??**) shows that the frequency shifts of the Stokes wave is dependent on the scattering angle θ. This shift is known as Brillouin frequency shift.

In optical fibers, depending on the incident wave, the scattered wave is polarized forward or backward. According to Eq. (**??**), Brillouin frequency shift is 0 for forward scattering ($\theta = 0°$) and is peaked for backward

scattering ($\theta = 180°$). The Brillouin frequency shift of the backward scattered Stokes wave is expressed by Eq. (**??**). Since the acoustic wave propagates reversely to the incident wave, anti-Stokes waves can be obtained. The anti-Stokes wave has a frequency as high as υ_B,

$$\nu_B = \frac{\omega_B}{2\pi} = 2\frac{nV_A}{\lambda_0} \tag{5}$$

In Eq. (**??**), n is the refractive index of the fiber, υ_B is Brillouin frequency shift, V_A is the acoustic velocity, and λ_0 is the wavelength of the pump (incident) wave [6].

Brillouin frequency shift is dependent on temperature due to the refractive index change as shown in Eq. (**??**):

$$\frac{\partial \nu_B}{\partial T} = \frac{2}{\lambda_0}\left[V_A\frac{dn}{dT} + n\frac{dV_A}{dT}\right] \tag{6}$$

The temperature-dependent Brillouin shift can be found in the following equation:

$$\upsilon_B(T) = \upsilon_{B0} + \frac{d\upsilon_B}{dT}(T - T_0) \tag{7}$$

υ_{B0} is Brillouin frequency shift at the reference temperature T_0. According to the studies, Brillouin frequency shift is linearly dependent on the temperature. Accordingly, the above equation can be written as follows [24,25]:

$$\upsilon_B(T) = \upsilon_{B0} + C_T(T - T_0) \tag{8}$$

Here C_T is the frequency-temperature coefficient. This coefficient is determined by fiber structure, laser wavelength, and additional fiber cladding and shield [26]. Since it shows the temperature dependence of Brillouin frequency shift, Eq. (**??**) can be used as a basis for the temperature measurement [5].

3. Materials and methods

The basic structure of the Brillouin optical time domain reflectometry (BOTDR) technique is shown in Figure 3.

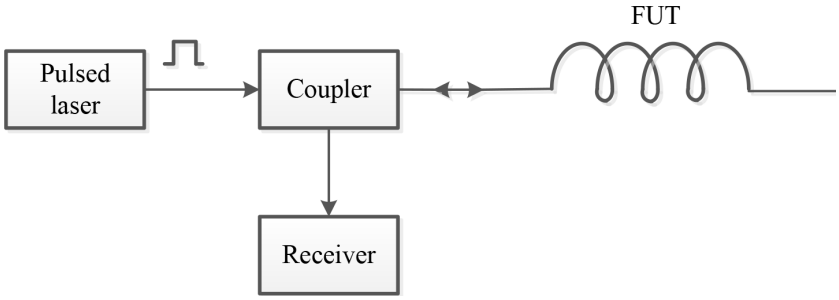

Figure 3. The basic structure of the BOTDR technique.

Similarly to optical time domain reflectometry (OTDR), which is used for the strength and length calculation of fiber optic cables, spontaneous Brillouin scattering is used in the BOTDR technique. In the fiber optic cable, the place of the measured ambient parameter, like strain and temperature, is defined by the calculation of the time interval between the pulsed laser light sent and back-scattered frequency.

The basic structure of the Brillouin optical time domain analysis (BOTDA) technique is shown in Figure 4.

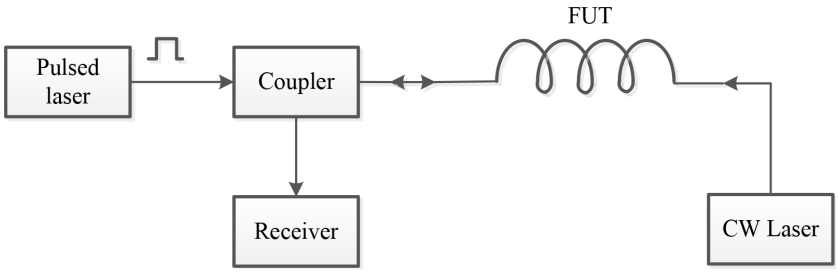

Figure 4. The basic structure of the BOTDA technique.

In the BOTDA technique, the raised Brillouin scattering method is used and the signal is generally implemented from both ends. Pulsed light and continuous wave are applied to the fiber optic cable from both ends. The frequency difference between these two signals is adjusted to Brillouin frequency shift. When the pulsed signal generates a loss, the continuous wave generates a gain. Thus, BOTDA can be obtained as a function of time.

In BOTDR, sending the signal from one side of the fiber is sufficient and this is the most important advantage of the BOTDR technique. Therefore, BOTDA is better according to the control, equipment used, and the signal processing technique.

3.1. Experimental setup and results

The experimental setup (BOTDR) for measuring Brillouin frequency shift at different ambient temperatures for a fixed length fiber under test (FUT) is shown in Figure 5.

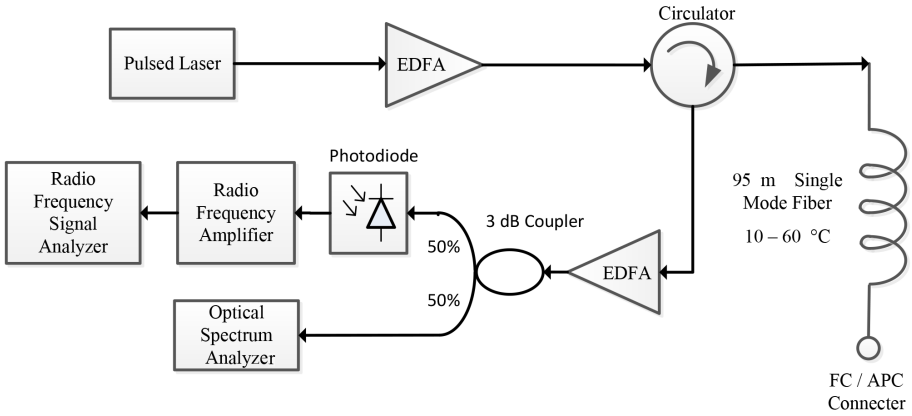

Figure 5. Setup for measuring Brillouin frequency shift at different ambient temperatures.

The laser source has 1553 nm wavelength, 50 ns pulse width, and 8.52 dBm gain. The incident wave leaving the laser has initially an 8 dBm gain. It is first sent to an erbium doped fiber amplifier (EDFA) to be amplified and then, through a circulator, it is sent to a 95-m length single mode FUT. The other end of the FUT is left open with the FC/APC connector being attached to reduce the return loss. The Brillouin scattering along the FUT is obtained through the circulator and is amplified by another EDFA. Then the amplified scattered wave is split into two by a 3-dB coupler and sent to a high-resolution optical spectrum analyzer (OSA) and a photodiode (PD). The electrical output of the photodiode is again amplified by a radio frequency amplifier (RFA) and finally analyzed by a radio frequency signal analyzer (RFSA).

First, a 95-m FUT is placed inside a furnace and heated up to 60 °C. After being kept at this temperature for a while, the Brillouin shift frequency value is measured through the 3rd outlet of the circulator by means of the RFSA. Then this step is repeated for the temperatures of 50 °C, 40 °C, 30 °C, 20 °C, and 10 °C. In order to ensure the uniform ambient temperature over the FUT, the furnace is set at a temperature for at least 30 min and only then the Brillouin frequency is read. The experiments were repeated with increasing temperature values of 10 °C to 60 °C. However, the same results were obtained. SBS variation is quite linear and stable, and it can be seen that similar graphics are obtained when the literature is examined [27–31]. The RFSA reading of Brillouin frequency for the 95-m single-mode FUT at the temperatures of 30 °C and 20 °C, respectively, is given in Figure 6.

Figure 7 shows the output of the optical spectrum for a 95-m test fiber. The first figure denotes the optical spectrum output at 20 °C and the others denote the optical spectrum output at the temperature of 40 °C and 60 °C, respectively. In Figure 7, signal 1 indicates Rayleigh scattering and signal 2 shows Stokes Brillouin scattering. The other signal indicates anti-Stokes Brillouin scattering. As can be seen in the figure, when temperature values increased, Brillouin shift also increased.

The Brillouin frequency shift values for each temperature are given in Figure 8.

As seen in Figure 8, the Brillouin frequency shift indeed has a linear dependence on the ambient temperature. Therefore, Eq. (**??**) can be defined for the amount of frequency shift and temperature.

By applying this formula, C_T is found to be $C_T = 0.93$ MHz/°C.

The BGS spectrum increases as the fiber length increases. Since the power of the lasers used at 1550 nm wavelength is low, fibers with a longer length should be used. Therefore, long fibers should be used in the determination of BGS. Since BGS is very weak it may not be measured in short fibers. In this study, the BGS spectrum was perceived with a short-length single mode fiber (SMF) by using the RF amplifier, EDFAs, and a high-resolution OSA differently from other publications. The results comparable with the literature are presented in the Table [27–31].

Table. Brillouin frequency shift measurements for different temperatures and fiber lengths in the literature.

Wavelength	Fiber	Fiber length	Temperature	BGS coefficient	References
1320 nm	GeO_2 doped core/pure-silica cladding fiber	250 m	–40 to 60 °C	1.17 MHz/°C	[27]
1320 nm	Pure-silica core/F-doped cladding	250 m	–40 to 60 °C	1.33 MHz/°C	[27]
1320 nm	GeO_2 core standard telecommunication fiber	200 m	–40 to 80 °C	1.36 MHz/°C	[28]
1310 nm	PM fiber type (Panda)	-	–5 to 45 °C	1.37 MHz/°C	[29]
1310 nm	PM fiber type (Bow-Tie)	-	–5 to 45 °C	2.30 MHz/°C	[29]
1310 nm	PM fiber type (Tiger)	-	–5 to 45 °C	1.66 MHz/°C	[29]
1550 nm	Dispersion-shifted fiber	110 m	20 to 850 °C	1.25 MHz/°C	[30]
1550 nm	SMF	2 km	–20 to 30 °C	1 MHz/°C	[31]
1553 nm	SMF	95 m	10 to 60 °C	0.93 MHz/°C	In this work

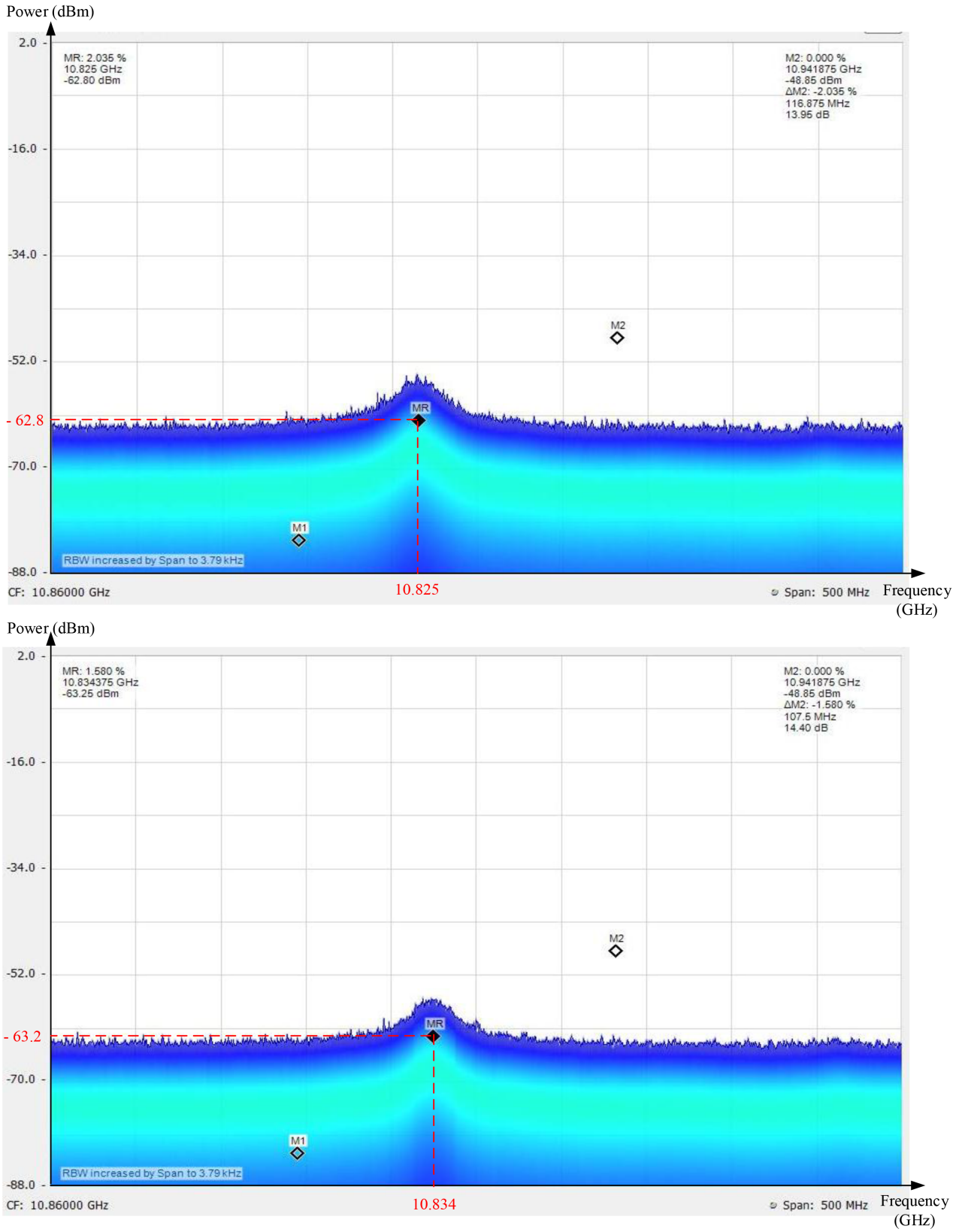

Figure 6. Brillouin frequency shift at 20 °C and 30 °C.

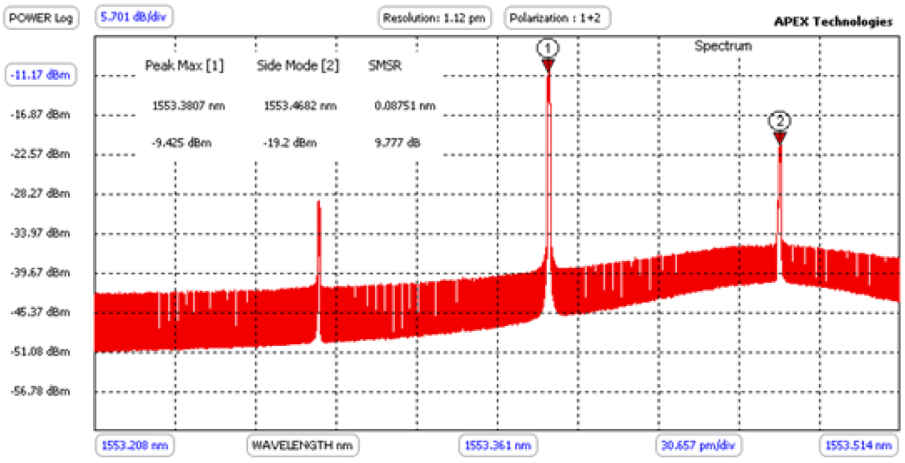

(a)

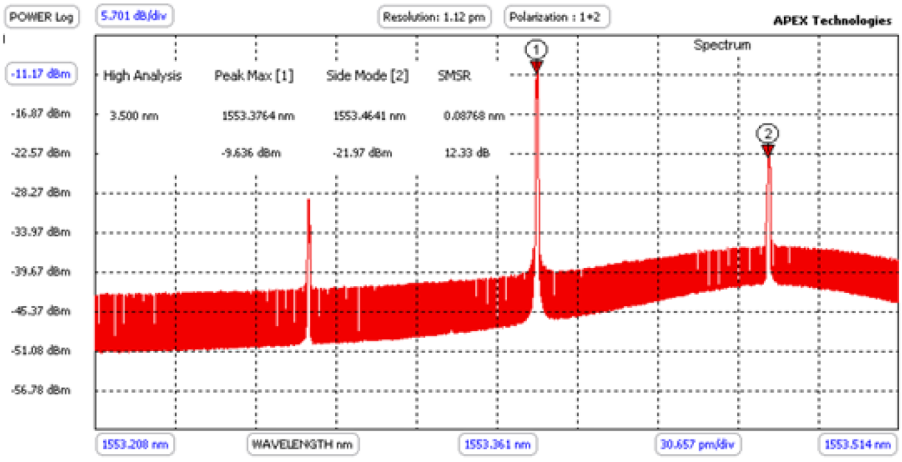

(b)

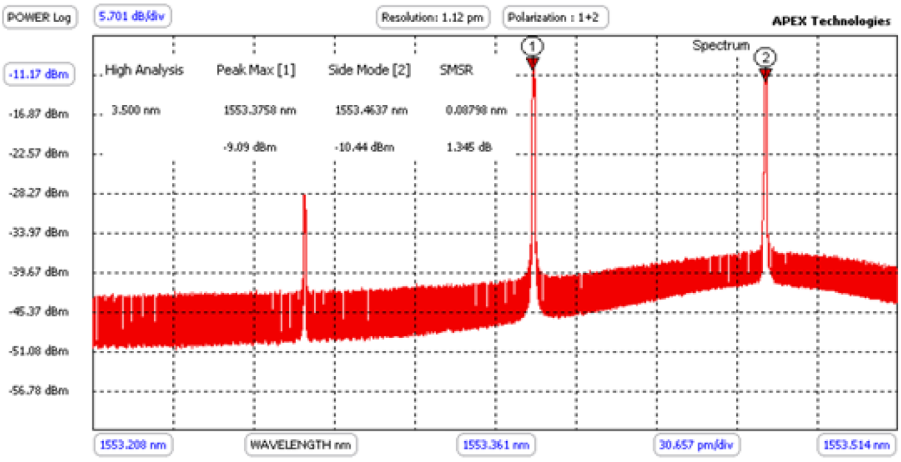

(c)

Figure 7. The output of the optical spectrum for 95-m-long test fiber (a) 20 °C (b) 40 °C (c) 60 °C.

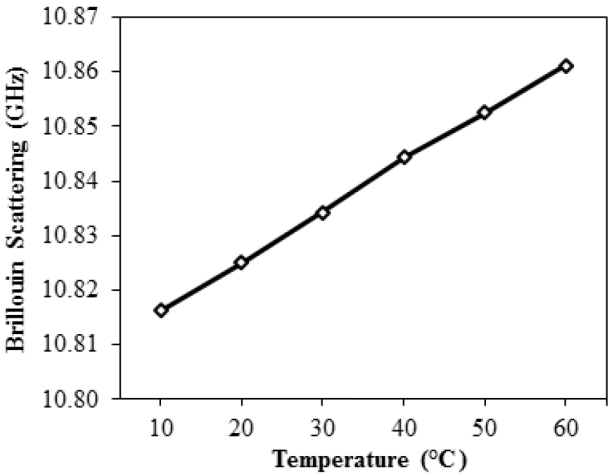

Figure 8. Brillouin frequency shift values for each temperature.

When the Table is examined, at least 2 km for conventional SMF, at least 200 m for doped SMF, and at least 110 m for different types of fibers are used. The BGS coefficient for this fiber length has been determined. In this study, BGS coefficient was obtained with 95 m classical SMF. This coefficient is closely related to the manufacturer and appears to be very close to the values obtained in the literature.

4. Conclusion

In this study, the BOTDR technique is used and the experimental observation of Brillouin scattering depending on the temperature change is analyzed. The fiber optic cable is exposed to different temperature changes and the frequency shift coefficient is obtained according to the Brillouin frequency shift. Consequently, by using this experimental method it is shown that the frequency change coefficient can be calculated for each type of fiber.

Acknowledgment

We thank the Scientific and Technological Research Council of Turkey (TÜBİTAK), for its support for the project entitled "Fiber Optic Sensing System Design and Development" with project number 5130044.

References

[1] Yücel M, Göktaş HH, Yücel M, Öztürk NF. The fiber optical sensing based on Brillouin scattering. In: IEEE 2014 Signal Processing and Communications Applications Conference; 23–25 April 2014; Trabzon, Turkey: IEEE. pp. 838-841.

[2] Yücel M, Yücel M, Öztürk NF, Göktaş HH. The analyzes of the Brillouin scattering for the different fiber types. In: IEEE 2015 Signal Processing and Communications Applications Conference; 16–19 May 2015; Malatya, Turkey: IEEE. pp. 632-635.

[3] Yücel M, Öztürk NF, Göktaş HH, Gemci C, Çelebi FV. The effects of signal level of the microwave generator on the Brillouin gain spectrum in BOTDA and BOTDR. 2015 WASET, Int J Electrical Comp Energetic Elec Com Eng 2015; 10: 23-27.

[4] Yücel M, Yücel M, Gündüz E, Göktaş HH, Öztürk NF. Using single-mode fiber as temperature sensor. In: IEEE 2016 Signal Processing and Communications Applications Conference; 16–19 May 2016; Zonguldak, Turkey: IEEE. pp. 461-464.

[5] Liu Z, Ferrier G, Bao X, Zeng X, Yu Q, Kim AK. Brillouin scattering based distributed fiber optic temperature sensing for fire detection. Fire Safe Sci 2003; 7: 221-232.

[6] Minardo A. Fiber-optic distributed strain/temperature sensors based on stimulated Brillouin scattering. PhD, Seconda Universita Degli Studi Di Napoli, Naples, Italy, 2012.

[7] Nath DK, Sugianto R, Finley D. Fiber-optic distributed-temperature-sensing technology. In: SPE 2006 Indian Drilling Technology Conference and Exhibition; 1–3 November 2006; Calgary, Alberta, Canada: SPE. pp. 9-18.

[8] Juarez JC, Taylor HF. Distributed fiber-optic intrusion sensor system. J Lightwave Technol 2005; 23: 2081-2087.

[9] Hartog AH, Payne DN. Remote measurement of temperature distribution using an optical fiber. In: 1982 European Conference on Optical Communication; 21–24 September 1982; Cannes, France: pp. 215-220.

[10] Dakin JP, Pratt DJ, Bibby GW, Ross JN. Distributed optical fiber Raman temperature sensor using a semiconductor light source and detector. IEEE Elec Lett 1985; 21: 569-570.

[11] Saxena MK, Raju S, Arya R, Ravindranath SVG, Kher S, Oak SM. Optical fiber distributed temperature sensor using short term Fourier transform based simplified signal processing of Raman signals. Measurement 2014; 47: 345-355.

[12] Challener WA. Multiparameter fiber optic sensing system for monitoring enhanced geothermal systems. General Electric Global Research, 2014.

[13] Horiguchi T, Kurashima T, Tateda M. Tensile strain dependence of Brillouin frequency shift in silica optical fibers. IEEE Photon Tech L 1989; 5: 107-108.

[14] Culverhouse D, Farahi F, Pannell CN, Jackson DA. Potential of stimulated Brillouin scattering as sensing mechanism for distributed temperature sensors. IEEE Elec Lett 1989; 14: 913-915.

[15] Huang S, Thévenaz L, Toyama K, Kim BY, Shaw HJ. Optical Kerr-effect in fiber-optic Brillouin ring laser gyroscopes. IEEE Photonic Tech L 1993; 3: 365-367.

[16] Siddiqui AS, Vienne GG. The effect of pump and signal laser fluctuations on the output signal for Raman and Brillouin optical fiber amplifiers. J Opt Comm 1992; 1: 33-36.

[17] Bao X, Webb DJ, Jackson DA. 22-km distributed sensor using Brillouin gain in an optical fiber. Opt Lett 1993; 7: 552-554.

[18] Thevenaz L, Nikles M, Fellay A, Facchini M, Robert P. Applications of distributed Brillouin fiber sensing. In: 1998 International Conference on Applied Optical Metrology; 29 September 1998; Balatonfured, Hungary: pp: 374-381.

[19] Kersey AD. A review of recent developments in fiber optic sensor technology. Opt Fiber Technol 1996; 2: 291-317.

[20] He J, Zhou Z, Ou J. Simultaneous measurement of strain and temperature using a hybrid local and distributed optical fiber sensing system. Measurement 2014; 47: 698-706.

[21] Wang Y, Wang C, Liang L. Measurement and analysis of high temperature using distributed fiber optic sensor. Int J Smart Sens Intel Sys 2014; 13: 19-20.

[22] Morgan A. New fire detection concepts with fibre optics technology. Fire Safe Eng 2000; 35-37.

[23] Maegerle R. Fire protection systems for traffic tunnels under test. Proceedings AUBE 2001; 1.

[24] Bao X, Brown A, DeMerchant M, Smith J. Characterization of the Brillouin-loss spectrum of single-mode fibers by use of very short ($<$10-ns) pulses. Opt Lett 1999; 8: 510-512.

[25] Garus D, Gogalla T, Krebber K, Schliep F. Brillouin optical-fiber frequency domain analysis for distributed temperature and strain measurements. J Lightwave Technol 1997; 4: 654-662.

[26] DeMerchant M. Distributed strain sensing for civil engineering applications. PhD, University of New Brunswick, New Brunswick, Canada, 2001.

[27] Kurashima T, Horiguchi T, Tateda M. Thermal effects of Brillouin gain spectra in single-mode fibers. IEEE Photon Tech L 1990; 10: 718-720.

[28] Nikles M, Thevenaz L, Philippe AR. Brillouin gain spectrum characterization in single-mode optical fibers. J Lightwave Technol 1997; 10: 1842-1851.

[29] Qinrong Y, Bao X, Liang C. Temperature dependence of Brillouin frequency, power, and bandwidth in panda, bow-tie, and tiger polarization-maintaining fibers. Opt Lett 2004; 1: 17-19.

[30] Yongqian L, Fucai Z, Yujun H, Zhi Y, Toshihiko Y. Advances in Brillouin-based distributed optical fiber temperature sensing. In: 2005 International Society for Optics and Photonics; 28 February 2005; Beijing, China: pp. 232-240.

[31] Kurashima T, Horiguchi T, Izumita H, Tateda M, Koyamada Y. Distributed strain measurement using BOTDR improved by taking account of temperature dependence of Brillouin scattering power. In: 1997 11th International Conference on Integrated Optics and Optical Fibre Communications and 23rd European Conference on Optical Communications; 22–25 September 1997; Edinburgh, UK: pp. 119-122.